J. Fluid Mech. (1978), *vol.* 87, *part* 4, *pp.* 673–694
Printed in Great Britain

The effect of two plane walls on the motion of a small sphere in a viscous fluid

By OSAMU SANO AND HIDENORI HASIMOTO
Department of Physics, Faculty of Science, University of Tokyo, Japan

(Received 30 September 1977)

A theoretical study is made of the motion of a small sphere in an incompressible viscous fluid bounded by two plane walls. The analysis is based on the Stokes equations of motion and the method of reflexions is employed to obtain the lowest-order wall effect on the sphere, which is allowed either to rotate or not as it translates in an arbitrary direction. The effect of two plane walls on the force and torque (or angular velocity) experienced by the sphere is not accurately estimated by superposing the contributions from the two individual walls.

1. Introduction

The presence of a boundary wall has great influence on the sedimentation of a particle or on the transport of suspensions, which motivates the study of wall effects. Although there have been many investigations of wall effects mostly on the basis of the Stokes equations of motion, the wall geometries so far considered have been limited to relatively simple ones such as a single plane wall (Lorentz 1907), two parallel plane walls (Faxén 1921, 1922; Ho & Leal 1974) and a cylindrical wall (Ladenburg 1907; Brenner & Happel 1958). The induced force and torque exerted on the sphere in these cases are expressed as series expansions in a small parameter $\epsilon = a/d$, where a is the sphere radius and d is the distance of the sphere from the wall. The sphere undergoes additional drag of order ϵ, but within the framework of the Stokes approximation it does not experience a side force when it translates parallel to or perpendicular to these walls. A detailed survey of wall effects is found in chapter 7 of Happel & Brenner (1973).

In practical applications, however, it often happens that the geometry of the wall is not so simple as that mentioned above. For example, consider a sedimenting sphere in a fluid bounded by two plane walls intersecting at a right angle, one of the walls being parallel to and the other perpendicular to the direction of motion. If we calculate the wall effect by superposing the contribution from the two individual walls, we come to the conclusion that the sphere does not undergo a side force, which is not correct even in the regime of the Stokes approximation. Analysis that takes into account the presence of both plane walls simultaneously is thus needed to give accurate results, and at the same time to make clear to what extent the conventional estimation is relevant.

Recently the effect of two plane walls was analysed by the present authors for the following two cases: (i) the force acting on a sphere when it translates in a viscous fluid bounded by two perpendicular plane walls (Sano & Hasimoto 1976), and (ii) the force and torque experienced by a sphere which moves on and across the bisector of

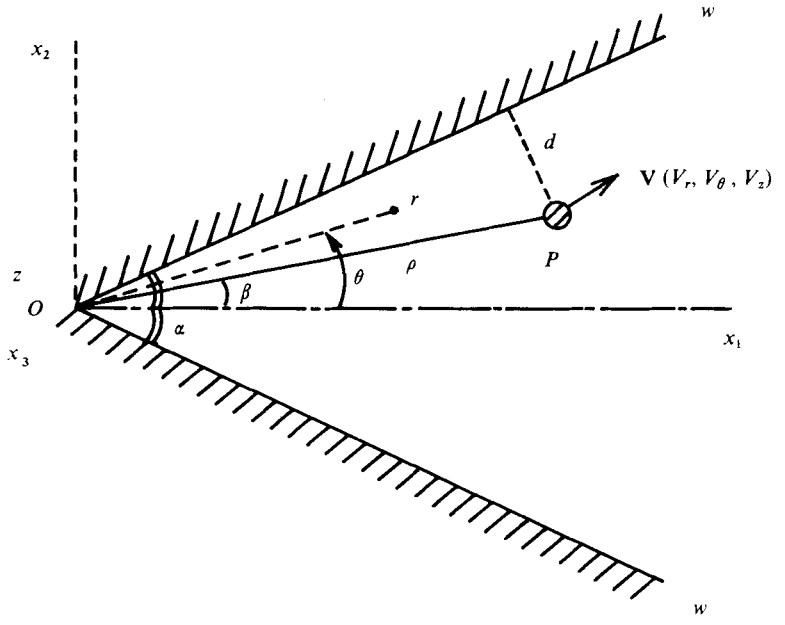

FIGURE 1. Definition sketch for a sphere and two plane walls.

the wedge containing a viscous fluid, with special attention to the asymptotic behaviour as the wedge angle reduces to zero (Sano & Hasimoto 1977). We used the method of reflexions to obtain the lowest-order wall effect on the assumption that ϵ was sufficiently small. In the analysis, we have used the general solution of the Stokes equations of motion (Imai 1973) and reduced the whole problem to a mixed boundary-value problem determining at most four harmonic functions. Using similar techniques, Hasimoto (1976) determined the first-order wall effect on a sphere moving in any direction inside a cylinder, as did Kim (1976) for a sphere translating along the axis of a right circular cone.

This paper is a generalization of the two-plane-wall-effect problem, and deals with the slow motion of a sphere in a viscous fluid contained in a wedge-shaped boundary. General expressions for the force and torque (when the sphere is kept from rotating) up to order ϵ and ϵ^2, respectively, are given in §§ 3 and 4. The sphere generally experiences a side force of order ϵ as well as a drag force, but there exist three principal axes of translation (i.e. the axes along which the sphere undergoes no lateral force) at any position of the fluid domain. The sphere also undergoes a torque of order ϵ^2, and there exists one axis, which we shall term the torque-free direction, such that if the sphere translates along this direction it does not suffer a torque. The principal axes of translation and the torque-free direction are considered in § 5. In § 6, we shall give alternative expressions in terms of ϵ^* ($= a/\rho$), where ρ is the distance between the sphere and the vertex of the wedge. When the sphere is allowed to rotate freely, the analysis developed in the foregoing sections remains unchanged for the calculation of the induced force, and in addition it leads directly to the determination of the angular velocity of the sphere as far as the lowest-order approximation is concerned. We shall show this in § 7, and the quantities that are possibly connected with observations are also discussed there.

2. Formulation of the problem and the method of solution

We consider the slow translational motion of a small sphere of radius a in an otherwise quiescent incompressible fluid of viscosity μ which is confined between two plane walls. We take Cartesian co-ordinates (x_1, x_2, x_3) so that the x_3 axis coincides with the edge, and so that the x_1 axis lies on the bisector of the wedge (see figure 1). We also introduce cylindrical co-ordinates (r, θ, z), where the z axis and the $\theta = 0$ plane correspond to the x_3 axis and the $x_2 = 0$ plane, respectively. In the following, we use two co-ordinate systems, and components are distinguished when necessary by the suffixes 1, 2, 3 or r, θ, z according as they are referred to the Cartesian co-ordinates or cylindrical co-ordinates. We denote the centre of the sphere by $P(r = \rho, \theta = \beta, z = 0)$, its velocity by $\mathbf{V} = (V_r, V_\theta, V_z)$, and the two plane walls W by $\theta = \pm\alpha$, where α is less than $\frac{1}{2}\pi$. The Reynolds number of the fluid motion is assumed to be sufficiently small for the inertia forces to be neglected. Consequently the governing equations and boundary conditions for the velocity $\mathbf{v} = (v_1, v_2, v_3)$ and pressure p in the fluid are

$$\mu\nabla^2\mathbf{v} = \nabla p, \quad \nabla . \mathbf{v} = 0, \tag{2.1), (2.2}$$

$$\mathbf{v} = 0 \text{ at infinity and on the walls,} \tag{2.3a, b}$$

$$\mathbf{v} = \mathbf{V} \text{ on the surface of the sphere.} \tag{2.3c}$$

We first assume that the sphere is not allowed to rotate, but this restriction will be removed later.

As a general solution of (2.1) and (2.2), we adopt the expressions (Imai 1973, p. 313)

$$\begin{aligned} &\mathbf{v} = \nabla(\mathbf{x} . \boldsymbol{\phi} + \phi_4) - 2\boldsymbol{\phi}, \quad p = 2\mu\nabla . \boldsymbol{\phi}, \\ &\boldsymbol{\phi} = (\phi_1, \phi_2, \phi_3), \quad \mathbf{x} = (x_1, x_2, x_3), \end{aligned} \tag{2.4}$$

where $\mathbf{x}$ is the position vector of the particle, and ϕ_n $(n = 1, \ldots, 4)$ are harmonic functions.

In order to fulfil the conditions (2.3), we use the method of reflexions and find a solution of the form

$$\mathbf{v} = \sum_{n=1}^{\infty} \mathbf{v}^{(n)}, \quad p = \sum_{n=1}^{\infty} p^{(n)}, \tag{2.5}$$

where each term $(\mathbf{v}^{(n)}, p^{(n)})$ separately satisfies (2.1) and (2.2). In this iteration scheme, one finds first the flow fields $(\mathbf{v}^{(1)}, p^{(1)})$ due to the particle as if the walls were absent, then adds the second reflexion $(\mathbf{v}^{(2)}, p^{(2)})$ which cancels the velocity on the walls induced by the initial fields, and then follow the third reflexion, the fourth reflexion, etc., satisfying the boundary conditions on the particle and on the walls alternately. Thus the solution amounts to a series expansion in ascending powers of ϵ, where ϵ is the ratio of the sphere radius to its characteristic separation distance from the boundary wall. In our present analysis, however, we shall confine ourselves to obtaining the first-order approximation to the force and torque experienced by the sphere, on the assumption that ϵ is sufficiently small. Then we are allowed to employ the point force approximation in determining the second reflexion. This approximation is based on the fact that at a large distance from any translating particle the velocity field must be asymptotically equal to that generated by a point force or a Stokeslet situated at the centre

of the particle, whose strength and direction are determined from the particle velocity, shape and dimension. Once the reflected fields $(\mathbf{v}^{(2)}, p^{(2)})$ are given, we can evaluate the force and torque acting on the sphere, correct to first order in the wall effect, by means of the generalized Faxén's law (Brenner 1962, 1964):

$$\mathbf{F} = -6\pi\mu a(\mathbf{V} - \mathbf{v}^{(2)} + \ldots)_P, \quad \mathbf{T} = 8\pi\mu a^3(\tfrac{1}{2}\nabla \times \mathbf{v}^{(2)} + \ldots)_P, \tag{2.6}$$

where the subscript P implies that the field is evaluated at the centre of the particle. Since the equations and boundary conditions are linear, we deal separately with the motion of a sphere in the two cases of translation parallel to the z axis (§ 3), and translation in the plane perpendicular to the z axis (§ 4).

3. Translation of a sphere parallel to both walls

We first consider the translational motion of a sphere with velocity V_z in the z direction. The first-order velocity field $\mathbf{v}^{(1)}$ is the flow due to the motion of a sphere in an unbounded domain. At a large distance from the sphere we approximate this field by that of a Stokeslet which is represented by

$$\phi_1^{(1)} = \phi_2^{(1)} = \phi_4^{(1)} = 0, \quad \phi_3^{(1)} = \chi, \tag{3.1}$$

where

$$\chi = -c_z/R, \quad c_z = (\tfrac{3}{4})aV_z, \quad R^2 = \rho^2 + r^2 - 2\rho r\cos(\theta - \beta) + z^2.$$

Then the reflected field $\mathbf{v}^{(2)}$, described by harmonic functions $\phi_n^{(2)}$ $(n = 1, \ldots, 4)$ regular in the flow field, must satisfy the following boundary conditions on the walls:

$$\left(r\frac{\partial}{\partial r} - 1\right)(\phi_1\cos\theta + \phi_2\sin\theta) + z\frac{\partial}{\partial r}\phi_3 + \frac{\partial}{\partial r}\phi_4 = -z\frac{\partial}{\partial r}\chi,$$

$$\cos\theta\frac{\partial}{\partial\theta}\phi_1 + \sin\theta\frac{\partial}{\partial\theta}\phi_2 + \phi_1\sin\theta - \phi_2\cos\theta + \frac{z}{r}\frac{\partial}{\partial\theta}\phi_3 + \frac{1}{r}\frac{\partial}{\partial\theta}\phi_4 = -\frac{z}{r}\frac{\partial}{\partial\theta}\chi,$$

$$r\frac{\partial}{\partial z}(\phi_1\cos\theta + \phi_2\sin\theta) + \left(z\frac{\partial}{\partial z} - 1\right)\phi_3 + \frac{\partial}{\partial z}\phi_4 = -\left(z\frac{\partial}{\partial z} - 1\right)\chi,$$

$$\text{at} \quad \theta = \pm\alpha, \tag{3.2}$$

where and hereafter in this section we omit the superscript (2) in the harmonic functions $\phi_n^{(2)}$. These requirements are fulfilled by choosing

$$\phi_1\cos\theta + \phi_2\sin\theta = 0, \quad \phi_3 = -\chi, \quad \phi_4 = 0,$$

$$\cos\theta\frac{\partial}{\partial\theta}\phi_1 + \sin\theta\frac{\partial}{\partial\theta}\phi_2 + \phi_1\sin\theta - \phi_2\cos\theta + \frac{z}{r}\frac{\partial}{\partial\theta}\phi_3 = -\frac{z}{r}\frac{\partial}{\partial\theta}\chi \quad \text{at} \quad \theta = \pm\alpha. \tag{3.3}$$

We now use the Fourier transform with respect to z:

$$F(r,\theta,k) = \int_{-\infty}^{\infty} dz\exp(\mathrm{i}kz)f(r,\theta,z) \equiv \mathscr{F}[f], \tag{3.4}$$

and the Kontrovich–Lebedev transform (Erdélyi *et al.* 1954) with respect to r:

$$\tilde{F}(\nu,\theta,k) = \int_0^{\infty} dr\, r^{-1}K_{\mathrm{i}\nu}(|k|\,r)F(r,\theta,k) \equiv \mathscr{K}[F], \tag{3.5}$$

where $K_{i\nu}(|k|r)$ is the modified Bessel function of imaginary order i_ν. Then the harmonic functions and boundary conditions mentioned above are transformed as follows:

$$(d^2/d\theta^2 - \nu^2)\tilde{\Phi}_n = 0 \quad (n = 1, \ldots, 4); \tag{3.6}$$

$$\tilde{\Phi}_1(\theta)\cos\theta + \tilde{\Phi}_2(\theta)\sin\theta = 0, \quad \tilde{\Phi}_3(\theta) = -\tilde{\chi}(\theta), \quad \tilde{\Phi}_4(\theta) = 0,$$

$$\tilde{\Phi}_1'(\theta)\cos\theta + \tilde{\Phi}_2'(\theta)\sin\theta + \tilde{\Phi}_1(\theta)\sin\theta - \tilde{\Phi}_2(\theta)\cos\theta + \mathscr{K}[\mathscr{F}[z\phi_3'/r]] = -\mathscr{K}[\mathscr{F}[z\chi'/r]]$$
$$\text{at} \quad \theta = \pm\alpha, \tag{3.7}$$

where the primes denote derivatives with respect to θ.

Solutions of (3.6) which satisfy the boundary conditions (3.7) are

$$\tilde{\Phi}_n = A_n \sinh\theta\nu + B_n \cosh\theta\nu \quad (n = 1, \ldots, 4); \tag{3.8}$$

where
$$A_1 = \frac{C^A}{\Delta^+(\nu;\alpha)}\sin\alpha\cosh\alpha\nu, \quad B_1 = \frac{C^S}{\Delta^-(\nu;\alpha)}\sin\alpha\sinh\alpha\nu,$$

$$A_2 = \frac{-C^S}{\Delta^-(\nu;\alpha)}\cos\alpha\cosh\alpha\nu, \quad B_2 = \frac{-C^A}{\Delta^+(\nu;\alpha)}\cos\alpha\sinh\alpha\nu,$$

$$A_3 = -\frac{2\pi c_z}{\nu\sinh\pi\nu}\frac{\sinh\beta\nu\sinh[(\pi-\alpha)\nu]}{\sinh\alpha\nu}K_{i\nu}(|k|\rho),$$

$$B_3 = -\frac{2\pi c_z}{\nu\sinh\pi\nu}\frac{\cosh\beta\nu\cosh[(\pi-\alpha)\nu]}{\cosh\alpha\nu}K_{i\nu}(|k|\rho),$$

$$A_4 = B_4 = 0,$$

with

$$C^A = \frac{8\pi c_z \operatorname{sgn} k}{i\nu D^-(\nu;\alpha)}\operatorname{Im}\left\{\left(k\frac{\partial}{\partial k} + 1 + i\nu\right)(p^A + iq^A)K_{i(\nu-1)}(|k|\rho)\right\},$$

$$C^S = \frac{8\pi c_z \operatorname{sgn} k}{i\nu D^+(\nu;\alpha)}\operatorname{Im}\left\{\left(k\frac{\partial}{\partial k} + 1 + i\nu\right)(p^S + iq^S)K_{i(\nu-1)}(|k|\rho)\right\},$$

$$p^A = \cos\alpha\sinh\alpha\nu\cos\beta\sinh\beta\nu + \sin\alpha\cosh\alpha\nu\sin\beta\cosh\beta\nu,$$
$$q^A = \sin\alpha\cosh\alpha\nu\cos\beta\sinh\beta\nu - \cos\alpha\sinh\alpha\nu\sin\beta\cosh\beta\nu,$$
$$p^S = \cos\alpha\cosh\alpha\nu\cos\beta\cosh\beta\nu + \sin\alpha\sinh\alpha\nu\sin\beta\sinh\beta\nu,$$
$$q^S = \sin\alpha\sinh\alpha\nu\cos\beta\cosh\beta\nu - \cos\alpha\cosh\alpha\nu\sin\beta\sinh\beta\nu,$$

and
$$\Delta^\pm(\nu;\alpha) = \sinh 2\alpha\nu \pm \nu\sin 2\alpha, \quad D^\pm(\nu;\alpha) = \cosh 2\alpha\nu \pm \cos 2\alpha. \tag{3.9}$$

By applying the inverse transform

$$f(r,\theta,z) = \frac{1}{\pi^3}\int_{-\infty}^{\infty} dk \exp(-ikz)\int_0^\infty d\nu\,\nu\sinh\pi\nu K_{i\nu}(|k|r)\tilde{F}(\nu,\theta,k) \tag{3.10}$$

to (3.8) we obtain the ϕ_n and the complete velocity field is determined through (2.4).

The force **F** and the torque **T** up to the first-order wall effect are now evaluated by means of (2.6). They are

$$\mathbf{F}/6\pi\mu a V_z = -[1 + \epsilon f_{zz}(\alpha,\beta)]\,\mathbf{e}_z + O(\epsilon^2), \tag{3.11}$$

$$\mathbf{T}/8\pi\mu a^2 V_z = -\epsilon^2[t_{rz}(\alpha,\beta)\,\mathbf{e}_r + t_{\theta z}(\alpha,\beta)\,\mathbf{e}_\theta] + O(\epsilon^4), \quad \epsilon = a/d, \quad d = \rho\sin|\alpha-\beta|, \tag{3.12}$$

where $\mathbf{e}_r$, $\mathbf{e}_\theta$ and $\mathbf{e}_z$ are the unit vectors in the r, θ and z directions. Here the functions f_{zz}, t_{rz} and $t_{\theta z}$ are

$$f_{zz} = \tfrac{3}{4}\sin|\alpha-\beta|\int_0^\infty d\nu\left\{1+\tanh\pi\nu\left[-M_0+2(\nu^2+\tfrac{1}{4})\left(\frac{(q^A)^2}{\Delta^+(\nu;\alpha)\,D^-(\nu;\alpha)}\right.\right.\right.$$

$$\left.\left.\left.+\frac{(q^S)^2}{\Delta^-(\nu;\alpha)\,D^+(\nu;\alpha)}\right)\right]\right\}, \quad M_0 = (\cosh 2\alpha\nu - \cosh 2\beta\nu)/\sinh 2\alpha\nu, \tag{3.13}$$

$$t_{rz} = \tfrac{3}{4}\sin^2(\alpha-\beta)\int_0^\infty d\nu\tanh\pi\nu\left[M_1-2(\nu^2+\tfrac{1}{4})\left(\frac{q^A\cdot r^A}{\Delta^+(\nu;\alpha)\,D^-(\nu;\alpha)}\right.\right.$$

$$\left.\left.+\frac{q^S\cdot r^S}{\Delta^-(\nu;\alpha)\,D^+(\nu;\alpha)}\right)\right], \quad M_1 = \nu\sinh 2\beta\nu/\sinh 2\alpha\nu, \tag{3.14}$$

$$t_{\theta z} = \tfrac{3}{4}\sin^2(\alpha-\beta)\int_0^\infty d\nu\left\{\tfrac{1}{2}-\tanh\pi\nu\left[\tfrac{1}{2}M_0+2(\nu^2+\tfrac{1}{4})\left(\frac{(q^A)^2}{\Delta^+(\nu;\alpha)\,D^-(\nu;\alpha)}\right.\right.\right.$$

$$\left.\left.\left.+\frac{(q^S)^2}{\Delta^-(\nu;\alpha)\,D^+(\nu;\alpha)}\right)\right]\right\}, \tag{3.15}$$

where

$$r^A = \sin\alpha\cosh\alpha\nu\sin\beta\sinh\beta\nu+\cos\alpha\sinh\alpha\nu\cos\beta\cosh\beta\nu,$$

$$r^S = \sin\alpha\sinh\alpha\nu\sin\beta\cosh\beta\nu+\cos\alpha\cosh\alpha\nu\cos\beta\sinh\beta\nu,$$

and other functions are defined in (3.9). Numerical values of f_{zz}, t_{rz} and $t_{\theta z}$ as functions of α and β are shown in figures 2–4. These results are the generalization of our previous calculations (Sano & Hasimoto 1976, 1977) which correspond to the case $\alpha = \frac{1}{4}\pi$ or $\beta = 0$. They also include all other works dealing with the motion of a sphere along a single plane wall (Lorentz 1907) or two parallel plane walls (Faxén 1921, 1922; Ho & Leal 1974).†

When a sphere moves parallel to both walls, it does not undergo a lateral force at any position in the region, in agreement with general considerations. The torque on the sphere, however, varies its direction as well as its magnitude with the location of the sphere. The deflexion angle δ, which is defined by the relation

$$\tan\delta = t_{\theta z}/t_{rz}, \tag{3.16}$$

is shown in figure 5; and an example of these directions for $\alpha = \frac{1}{6}\pi$ is given in figure 6. These figures show clearly how the sphere's direction varies from the θ direction on the bisector to the r direction near the wall. As the wall is approached the $O(\epsilon^2)$ coefficient of the torque reduces to zero, and the torque becomes of order ϵ^4 as obtained by Faxén (1921) for the case of a single plane wall:

$$T/8\pi\mu a^2 V_z = \tfrac{3}{32}\epsilon^4(1-\tfrac{3}{8}\epsilon), \tag{3.17}$$

which acts in the same direction as if it would make the sphere roll along the wall.

† In particular, when the sphere is situated midway between two plane walls ($\beta = 0$), the asymptotic forms of f and t as α goes to zero are

$$f_{zz} = 1{\cdot}004121+\alpha^2[\tfrac{27}{64}\ln\alpha+0{\cdot}005108]+\ldots, \quad t_{\theta z} = -0{\cdot}224330\alpha-\alpha^3[\tfrac{27}{64}\ln\alpha+0{\cdot}050810]+\ldots,$$

and those as α approaches to $\frac{1}{2}\pi$ are

$$f_{zz} = \tfrac{9}{16}+0{\cdot}3515(\tfrac{1}{2}\pi-\alpha)+\ldots, \quad t_{\theta z} = -0{\cdot}0703(\tfrac{1}{2}\pi-\alpha)+\ldots.$$

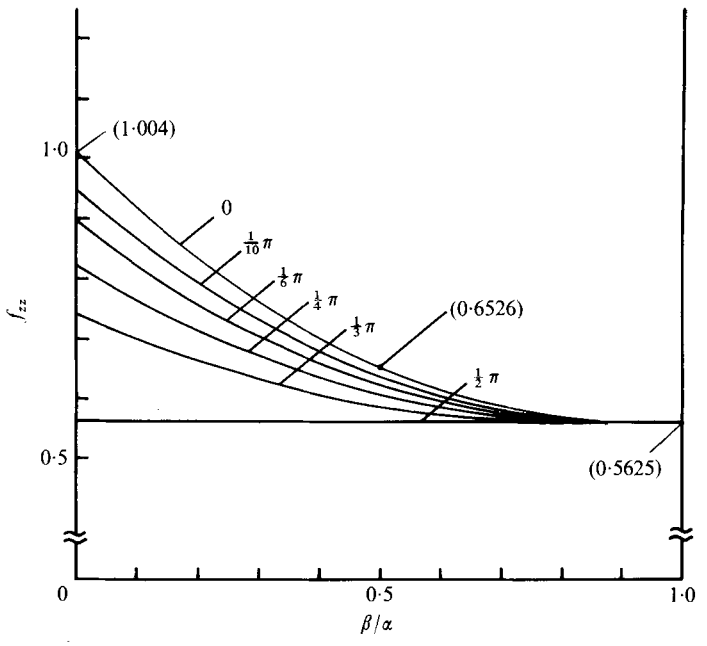

FIGURE 2. Graph of f_{zz} given by (3.13), which is the same as the additional principal drag λ_3 in (5.5), for different values of α. The values 1·004 and 0·6526 in parentheses are those obtained by Faxén (1922, 1921); the curves for $\alpha = \frac{1}{2}\pi$ and $\alpha = 0$ correspond to those deduced from Lorentz (1907) and Ho & Leal (1974), respectively.

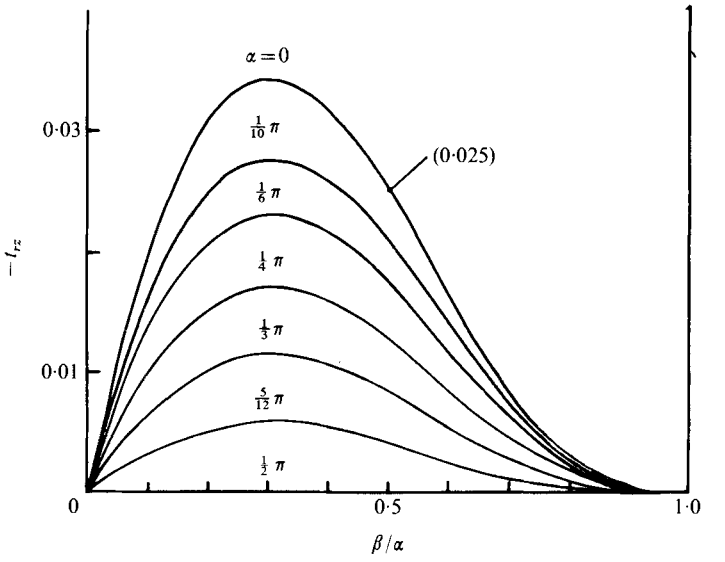

FIGURE 3. Graph of $-t_{rz}$ given by (3.14). The value 0·025 in parentheses is deduced from Faxén (1921) as well as Wakiya (1956); the curve for $\alpha = 0$ corresponds to Ho & Leal (1974).

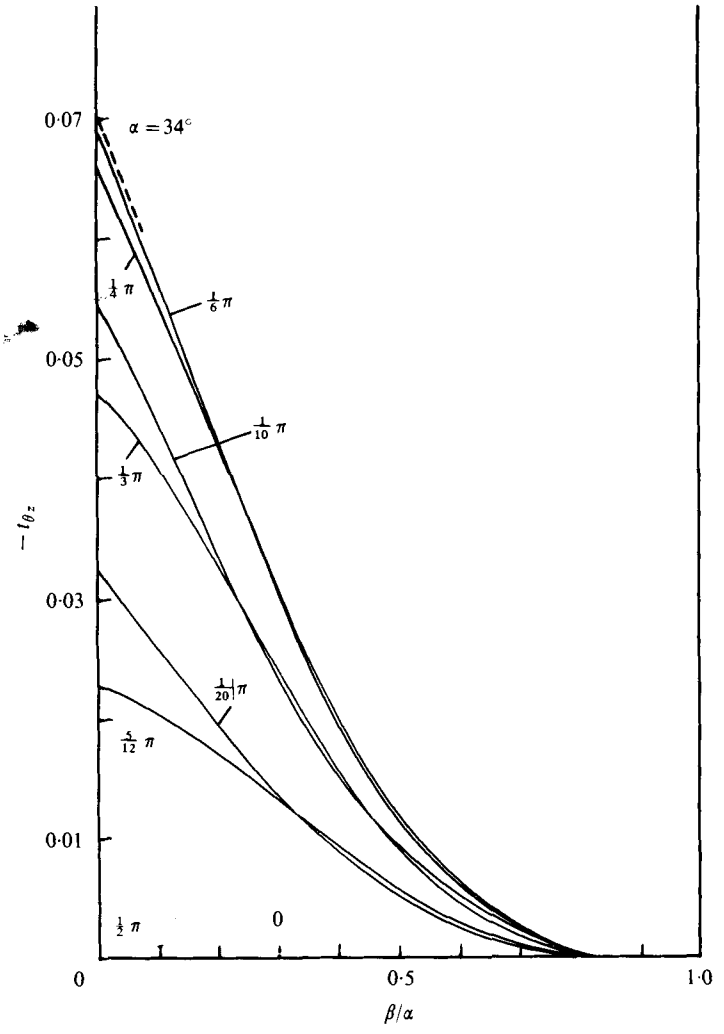

FIGURE 4. Graph of $-t_{\theta z}$ given by (3.15) for different values of α. Maximum value is obtained at $\alpha = 34°$ on the bisector.

4. Translation of a sphere perpendicular to the intersection of the walls

In this section we consider the translation of a sphere with velocity $\mathbf{U} = (V_r, V_\theta, 0)$. We denote the magnitude of the velocity by U, and the angle between V_r and V_θ by γ, i.e.

$$\tan\gamma = V_\theta/V_r. \tag{4.1}$$

The procedures for calculation are almost the same as those shown in the previous section. The asymptotic behaviour of the first-order velocity field $\mathbf{v}^{(1)}$ in this case is described by

$$\phi_1^{(1)} = \chi\cos(\beta+\gamma), \quad \phi_2^{(1)} = \chi\sin(\beta+\gamma), \quad \phi_3^{(1)} = 0, \quad \phi_4^{(1)} = -\rho\chi\cos\gamma, \tag{4.2}$$

where $\chi = -c/R$, $c = \frac{3}{4}aU$, $R^2 = \rho^2 + r^2 - 2\rho r\cos(\theta-\beta) + z^2$. We then introduce the

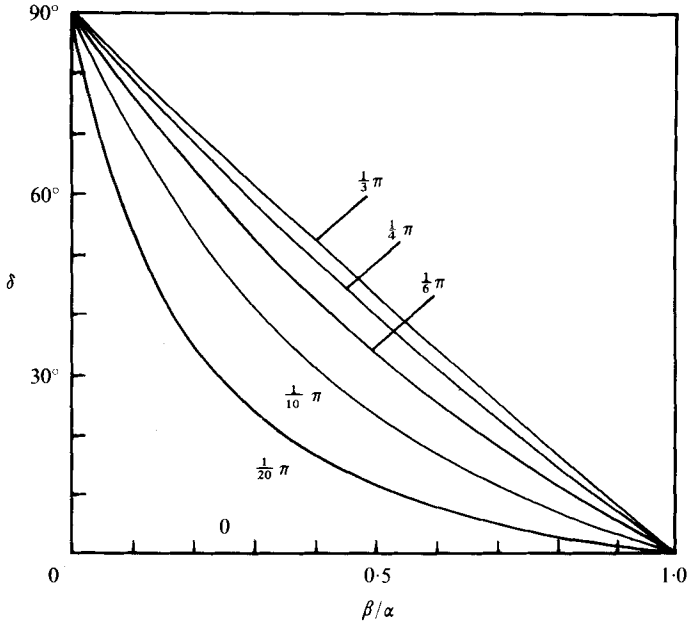

FIGURE 5. Graph of δ defined by (3.16) for different values of α.

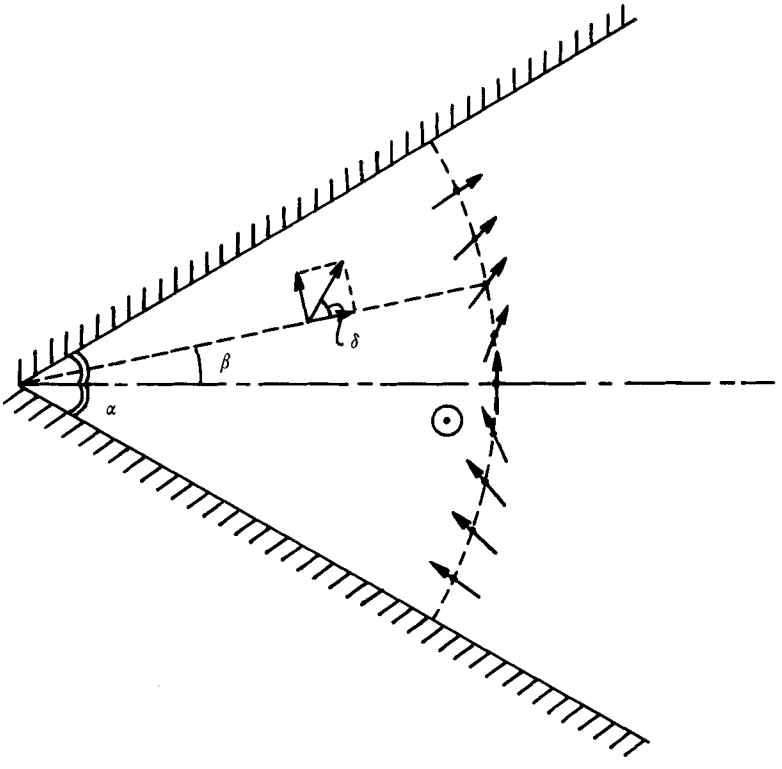

FIGURE 6. The direction of torque for $\alpha = \frac{1}{8}\pi$, where the sphere moves perpendicularly out of the paper. The magnitude of the torque $O(\epsilon^2)$ becomes zero in the vicinity of the wall, and the torque $o(\epsilon^4)$ takes its place.

reflected field $\mathbf{v}^{(2)}$, which is expressed by harmonic functions $\phi_n^{(2)}$. The boundary conditions for $\phi_n^{(2)}$ are

$$\left(r\frac{\partial}{\partial r}-1\right)(\phi_1\cos\theta+\phi_2\sin\theta)+z\frac{\partial}{\partial r}\phi_3+\frac{\partial}{\partial r}\phi_4$$
$$=-\cos(\theta-\beta-\gamma)\left(r\frac{\partial}{\partial r}-1\right)\chi+\rho\cos\gamma\frac{\partial}{\partial r}\chi,$$
$$\cos\theta\frac{\partial}{\partial\theta}\phi_1+\sin\theta\frac{\partial}{\partial\theta}\phi_2+\phi_1\sin\theta-\phi_2\cos\theta+\frac{z}{r}\frac{\partial}{\partial\theta}\phi_3+\frac{1}{r}\frac{\partial}{\partial\theta}\phi_4$$
$$=-\cos(\theta-\beta-\gamma)\frac{\partial}{\partial\theta}\chi-\chi\sin(\theta-\beta-\gamma)+\frac{\rho}{r}\cos\gamma\frac{\partial}{\partial\theta}\chi,$$
$$r\frac{\partial}{\partial z}(\phi_1\cos\theta+\phi_2\sin\theta)+\left(z\frac{\partial}{\partial z}-1\right)\phi_3+\frac{\partial}{\partial z}\phi_4$$
$$=-\cos(\theta-\beta-\gamma)r\frac{\partial}{\partial z}\chi+\rho\cos\gamma\frac{\partial}{\partial z}\chi \text{ on the walls } \theta=\pm\alpha, \quad (4.3)$$

where we have deleted the superscript (2) in the functions $\phi_n^{(2)}$. These conditions are fulfilled if we choose

$$\phi_1\cos\theta+\phi_2\sin\theta=-\chi\cos(\theta-\beta-\gamma),\quad \phi_4=\rho\chi\cos\gamma,\quad \phi_3=0,$$
$$\cos\theta\frac{\partial}{\partial\theta}\phi_1+\sin\theta\frac{\partial}{\partial\theta}\phi_2+\phi_1\sin\theta-\phi_2\cos\theta+\frac{1}{r}\frac{\partial}{\partial\theta}\phi_4$$
$$=-\cos(\theta-\beta-\gamma)\frac{\partial}{\partial\theta}\chi-\chi\sin(\theta-\beta-\gamma)+\frac{\rho}{r}\cos\gamma\frac{\partial}{\partial\theta}\chi \quad \text{at} \quad \theta=\pm\alpha. \quad (4.4)$$

After some calculation, we obtain the expressions for $\tilde{\Phi}_n$:

$$\tilde{\Phi}_n=A_n\sinh\theta\nu+B_n\cosh\theta\nu\ (n=1,2,4);\quad \tilde{\Phi}_3=0, \quad (4.5)$$

where
$$A_1=\frac{4\pi c}{\nu\sinh\pi\nu\,\Delta^+(\nu;\alpha)}[a_1^0K_{i\nu}(|k|\rho)+\mathrm{Re}\{a_1^+|k|\rho K_{i(\nu+1)}(|k|\rho)\}],$$
$$B_1=\frac{4\pi c}{\nu\sinh\pi\nu\,\Delta^-(\nu;\alpha)}[b_1^0K_{i\nu}(|k|\rho)+\mathrm{Re}\{b_1^+|k|\rho K_{i(\nu+1)}(|k|\rho)\}],$$
$$A_2=\frac{4\pi c}{\nu\sinh\pi\nu\,\Delta^-(\nu;\alpha)}[a_2^0K_{i\nu}(|k|\rho)+\mathrm{Re}\{a_2^+|k|\rho K_{i(\nu+1)}(|k|\rho)\}],$$
$$B_2=\frac{4\pi c}{\nu\sinh\pi\nu\,\Delta^+(\nu;\alpha)}[b_2^0K_{i\nu}(|k|\rho)+\mathrm{Re}\{b_2^+|k|\rho K_{i(\nu+1)}(|k|\rho)\}],$$
$$A_4=\frac{2\pi c\cos\gamma}{\nu\sinh\pi\nu}\frac{\sinh[(\pi-\alpha)\nu]\sinh\beta\nu}{\sinh\alpha\nu}\rho K_{i\nu}(|k|\rho),$$
$$B_4=\frac{2\pi c\cos\gamma}{\nu\sinh\pi\nu}\frac{\cosh[(\pi-\alpha)\nu]\cosh\beta\nu}{\cosh\alpha\nu}\rho K_{i\nu}(|k|\rho),$$

with

$$a_1^0=\nu\sin\alpha[\cos\alpha\cos(\beta+\gamma)\sinh\beta\nu\cosh\pi\nu+\sin\alpha\sin(\beta+\gamma)\cosh\beta\nu\sinh\pi\nu]$$
$$-\cos(\beta+\gamma)\cosh\alpha\nu\sinh[(\pi-\alpha)\nu]\sinh\beta\nu,$$

$$b_1^0 = \nu \sin\alpha[\cos\alpha\,\cos(\beta+\gamma)\,\cosh\beta\nu\,\cosh\pi\nu + \sin\alpha\,\sin(\beta+\gamma)\,\sinh\beta\nu\,\sinh\pi\nu] - \cos(\beta+\gamma)\,\sinh\alpha\nu\,\cosh[(\pi-\alpha)\nu]\,\cosh\beta\nu,$$

$$a_2^0 = -\nu\cos\alpha[\cos\alpha\,\cos(\beta+\gamma)\,\cosh\beta\nu\,\sinh\pi\nu + \sin\alpha\,\sin(\beta+\gamma)\,\sinh\beta\nu\,\cosh\pi\nu] - \sin(\beta+\gamma)\,\cosh\alpha\nu\,\sinh[(\pi-\alpha)\nu]\,\sinh\beta\nu,$$

$$b_2^0 = -\nu\cos\alpha[\cos\alpha\,\cos(\beta+\gamma)\,\sinh\beta\nu\,\sinh\pi\nu + \sin\alpha\,\sin(\beta+\gamma)\,\cosh\beta\nu\,\cosh\pi\nu] - \sin(\beta+\gamma)\,\sinh\alpha\nu\,\cosh[(\pi-\alpha)\nu]\,\cosh\beta\nu,$$

$$a_1^+ = -\mathrm{i}\sin\alpha\,\cos\gamma\,\cosh\alpha\nu\,\sinh[\beta(\nu+\mathrm{i})]\,\sinh\pi\nu/\sinh[\alpha(\nu+\mathrm{i})],$$

$$b_1^+ = -\mathrm{i}\sin\alpha\,\cos\gamma\,\sinh\alpha\nu\,\cosh[\beta(\nu+\mathrm{i})]\,\sinh\pi\nu/\cosh[\alpha(\nu+\mathrm{i})],$$

$$a_2^+ = \mathrm{i}\cos\alpha\,\cos\gamma\,\cosh\alpha\nu\,\cosh[\beta(\nu+\mathrm{i})]\,\sinh\pi\nu/\cosh[\alpha(\nu+\mathrm{i})],$$

$$b_2^+ = \mathrm{i}\cos\alpha\,\cos\gamma\,\sinh\alpha\nu\,\sinh[\beta(\nu+\mathrm{i})]\,\sinh\pi\nu/\sinh[\alpha(\nu+\mathrm{i})]. \tag{4.6}$$

The harmonic functions ϕ_n, which are obtained by applying the inverse transform to (4.5), together with $\mathbf{v}^{(1)}$ completely determine the velocity field in the domain under consideration.

The force $\mathbf{F}$ and the torque $\mathbf{T}$ on the sphere correct to first-order in the wall effect are calculated by means of the generalized Faxén law, and are

$$\mathbf{F}/6\pi\mu aU = -\cos\gamma\{[1+\epsilon f_{rr}(\alpha,\beta)]\,\mathbf{e}_r + \epsilon f_{r\theta}(\alpha,\beta)\,\mathbf{e}_\theta\} - \sin\gamma\{\epsilon f_{\theta r}(\alpha,\beta)\,\mathbf{e}_r + [1+\epsilon f_{\theta\theta}(\alpha,\beta)]\,\mathbf{e}_\theta\} + O(\epsilon^2), \tag{4.7}$$

$$\mathbf{T}/8\pi\mu a^2 U = -\epsilon^2[t_{zr}(\alpha,\beta) + t_{z\theta}(\alpha,\beta)]\,\mathbf{e}_z + O(\epsilon^4), \tag{4.8}$$

where

$$f_{rr} = \tfrac{3}{4}\sin|\alpha-\beta|\int_0^\infty d\nu\left\{1+\tanh\pi\nu\left[\tfrac{1}{2}M_0 + \tfrac{3}{4}\left(\frac{N_{rr}^+}{\Delta^+(\nu;\alpha)} + \frac{N_{rr}^-}{\Delta^-(\nu;\alpha)}\right) + 2\left(\frac{N_{rr}^A}{\Delta^+(\nu;\alpha)\,D^-(\nu;\alpha)} + \frac{N_{rr}^S}{\Delta^-(\nu;\alpha)\,D^+(\nu;\alpha)}\right)\right]\right\},$$

with

$$N_{rr}^\pm = \nu\cos 2\alpha\,\sin 2\beta\,\sinh 2\beta\nu - (\cosh 2\alpha\nu - \cosh 2\beta\nu) \pm \cos 2\beta(\cosh 2\alpha\nu\,\cosh 2\beta\nu - 1),$$

$$N_{rr}^A = q^A[3\nu p^A + (\nu^2 + \tfrac{7}{4})\,q^A],$$

$$N_{rr}^S = q^S[3\nu p^S + (\nu^2 + \tfrac{7}{4})\,q^S]; \tag{4.9}$$

$$f_{r\theta} = f_{\theta r} = \tfrac{3}{4}\sin|\alpha-\beta|\int_0^\infty d\nu\,(-\tfrac{3}{4})\tanh\pi\nu\left(\frac{N_{r\theta}^+}{\Delta^+(\nu;\alpha)} + \frac{N_{r\theta}^-}{\Delta^-(\nu;\alpha)}\right),$$

with

$$N_{r\theta}^\pm = \nu\sinh 2\beta\nu(1-\cos 2\alpha\,\cos 2\beta) \pm \sin 2\beta(\cosh 2\alpha\nu\,\cosh 2\beta\nu - 1); \tag{4.10}$$

$$f_{\theta\theta} = \tfrac{3}{4}\sin|\alpha-\beta|\int_0^\infty d\nu\left[1+\tfrac{1}{2}\tanh\pi\nu\left(\frac{N_{\theta\theta}^+}{\Delta^+(\nu;\alpha)} + \frac{N_{\theta\theta}^-}{\Delta^-(\nu;\alpha)}\right)\right],$$

with

$$N_{\theta\theta}^\pm = \nu^2[\cosh 2\beta\nu(1-\cos 2\alpha\,\cos 2\beta) \mp (\cos 2\alpha - \cos 2\beta)] \pm \nu\sin 2\beta\,\sinh 2\beta\nu(\cosh 2\alpha \mp \cos 2\alpha) - (\cosh 2\alpha\nu - \cosh 2\beta\nu) \mp \cos 2\beta(\cosh 2\alpha\nu\,\cosh 2\beta\nu - 1); \tag{4.11}$$

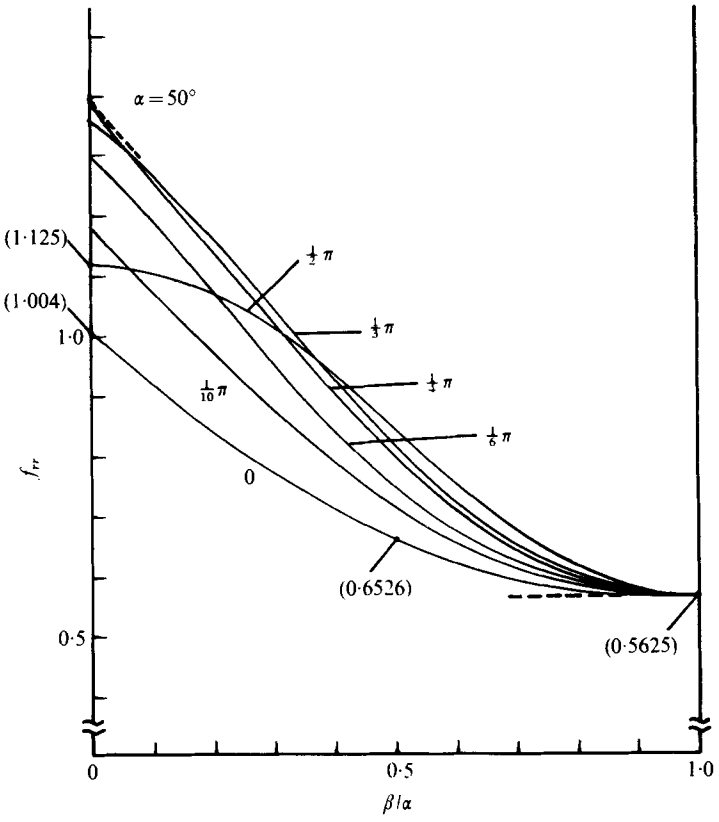

FIGURE 7. Graph of f_{rr} given by (4.9) for various α. The curves for $\alpha = \frac{1}{2}\pi$ and for $\alpha = 0$ are the same as those deduced from Lorentz (1907) and Ho & Leal (1974), respectively; the values 1·004 and 0·6526 in parentheses have been given by Faxén (1922, 1921). Maximum value is attained at $\alpha = 50°$ on the bisector.

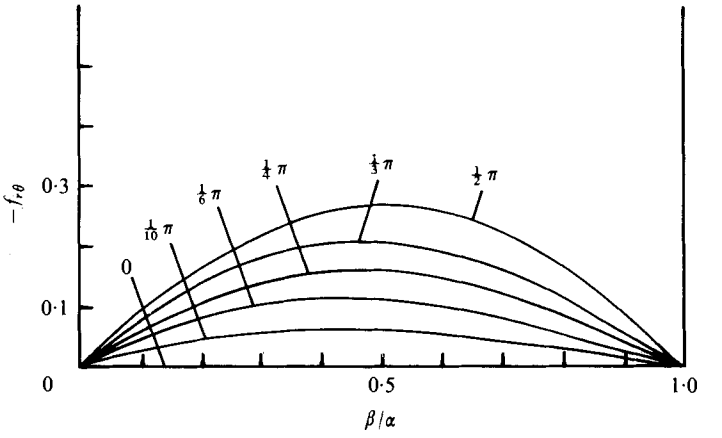

FIGURE 8. Graph of $-f_{r\theta}$ (or $-f_{\theta r}$) given by (4.10) for various α, where $\epsilon f_{r\theta}$ is the side force experienced by the sphere.

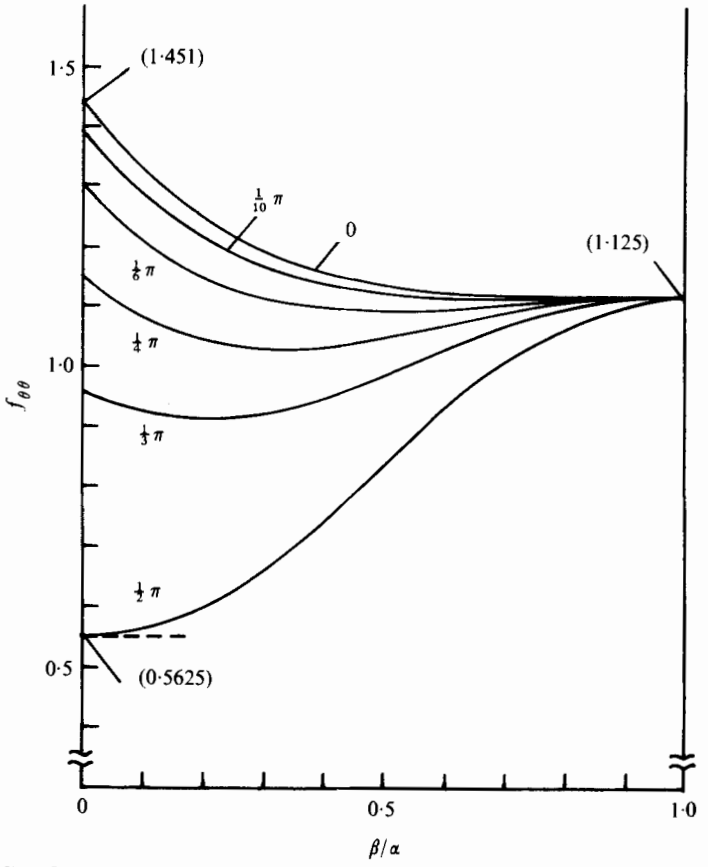

FIGURE 9. Graph of $f_{\theta\theta}$ given by (4.11) for various α. The curve for $\alpha = \frac{1}{2}\pi$ is deduced from Lorentz (1907), and the curve for $\alpha = 0$ including the value 1·451 in parentheses corresponds to Ho & Leal (1974).

$$t_{zr} = \tfrac{3}{4}\sin^2(\alpha-\beta)\int_0^\infty d\nu \tanh \pi\nu \left(\frac{\frac{1}{2}N_{zr}^+}{\Delta^+(\nu;\alpha)} + \frac{\frac{1}{2}N_{zr}^-}{\Delta^-(\nu;\alpha)} + \frac{2N_{zr}^A}{\Delta^+(\nu;\alpha)D^-(\nu;\alpha)} + \frac{2N_{zr}^S}{\Delta^-(\nu;\alpha)D^+(\nu;\alpha)}\right),$$

with

$$\begin{aligned} N_{zr}^\pm &= \nu^2 \sin 2\beta(\pm 1 - \cos 2\alpha \cosh 2\beta\nu) \\ &\quad - \nu \sinh 2\beta\nu[1 \pm \cos 2\beta \cosh 2\alpha\nu + \tfrac{1}{2}(1+\cos 2\alpha \cos 2\beta)] \\ &\quad \pm \tfrac{1}{2}\sin 2\beta(\cosh 2\alpha\nu \cosh 2\beta\nu - 1), \\ N_{zr}^A &= r^A[\nu p^A + (\nu^2+\tfrac{3}{4})q^A] - s^A(2\nu^2 p^A + \nu q^A), \\ N_{zr}^S &= r^S[\nu p^S + (\nu^2+\tfrac{3}{4})q^S] - s^S(2\nu^2 p^S + \nu q^S); \end{aligned} \tag{4.12}$$

and

$$t_{z\theta} = \tfrac{3}{4}\sin^2(\alpha-\beta)\int_0^\infty d\nu \left[-\tfrac{1}{2} + \tfrac{1}{4}\tanh \pi\nu \left(\frac{N_{z\theta}^+}{\Delta^+(\nu;\alpha)} + \frac{N_{z\theta}^-}{\Delta^-(\nu;\alpha)}\right)\right],$$

with

$$\begin{aligned} N_{z\theta}^\pm &= 2\nu^2[\cosh 2\beta\nu(1 - \cos 2\alpha \cos 2\beta) \mp (\cos 2\alpha - \cos 2\beta)] \\ &\quad \pm \nu \sin 2\beta \sinh 2\beta\nu(2\cosh 2\alpha\nu \pm \cos 2\alpha) \\ &\quad + \cosh 2\alpha\nu - \cosh 2\beta\nu \pm \cos 2\beta(\cosh 2\alpha\nu \cosh 2\beta\nu - 1). \end{aligned} \tag{4.13}$$

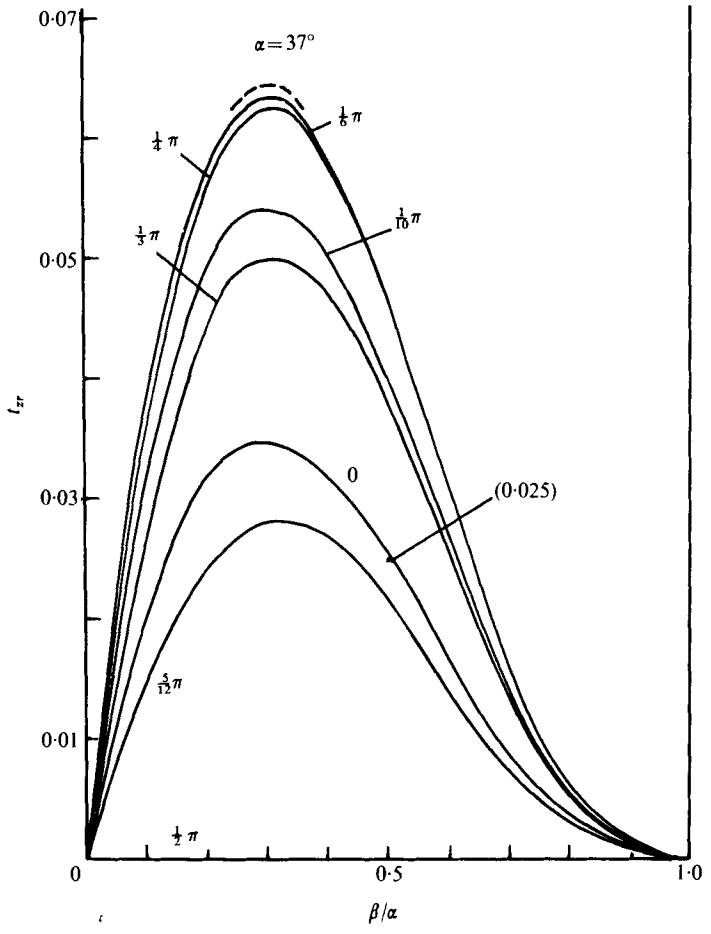

FIGURE 10. Graph of t_{zr} given by (4.12) for various α. The value 0·025 in parentheses is deduced from Faxén (1921) as well as Wakiya (1956); the curve for $\alpha = 0$ corresponds to Ho & Leal (1974). Maximum value is attained at $\alpha = 37°$ at an intermediate position.

In these expressions

$$s^A = \sin\alpha \cosh\alpha\nu \cos\beta \cosh\beta\nu - \cos\alpha \sinh\alpha\nu \sin\beta \sinh\beta\nu,$$
$$s^S = \sin\alpha \sinh\alpha\nu \cos\beta \sinh\beta\nu - \cos\alpha \cosh\alpha\nu \sin\beta \cosh\beta\nu,$$

and we again take minimum distance $d = \rho \sin|\alpha - \beta|$ as a characteristic length in defining the parameter $\epsilon = a/d$. Numerical values of f and t as functions of α and β are shown in figures 7–11, which again include the results for a single plane wall and two parallel plane walls as a special case.† The results show that, in general, a sphere experiences a force not only in the direction of motion but also in the direction perpendicular to it. This side force originates in the asymmetric boundary condition with

† In the case $\beta = 0$, the asymptotic forms of f and t as α goes to zero are
$f_{rr} = 1{\cdot}004121 + \alpha^2[-(\frac{1285}{644})\ln\alpha - 0{\cdot}951767] + \ldots$, $f_{\theta\theta} = 1{\cdot}451568 - 0{\cdot}510735\alpha^2 + \ldots$,
$t_{z\theta} = 0{\cdot}138044\alpha - 0{\cdot}084947\alpha^3 + \ldots$,
and those for α near $\frac{1}{2}\pi$ are
$f_{rr} = \frac{9}{8} + 0{\cdot}6330(\frac{1}{2}\pi - \alpha) + \ldots$, $f_{\theta\theta} = \frac{9}{16} + 0{\cdot}7031(\frac{1}{2}\pi - \alpha) + \ldots$, $t_{z\theta} = 0{\cdot}1406(\frac{1}{2}\pi - \alpha) + \ldots$.

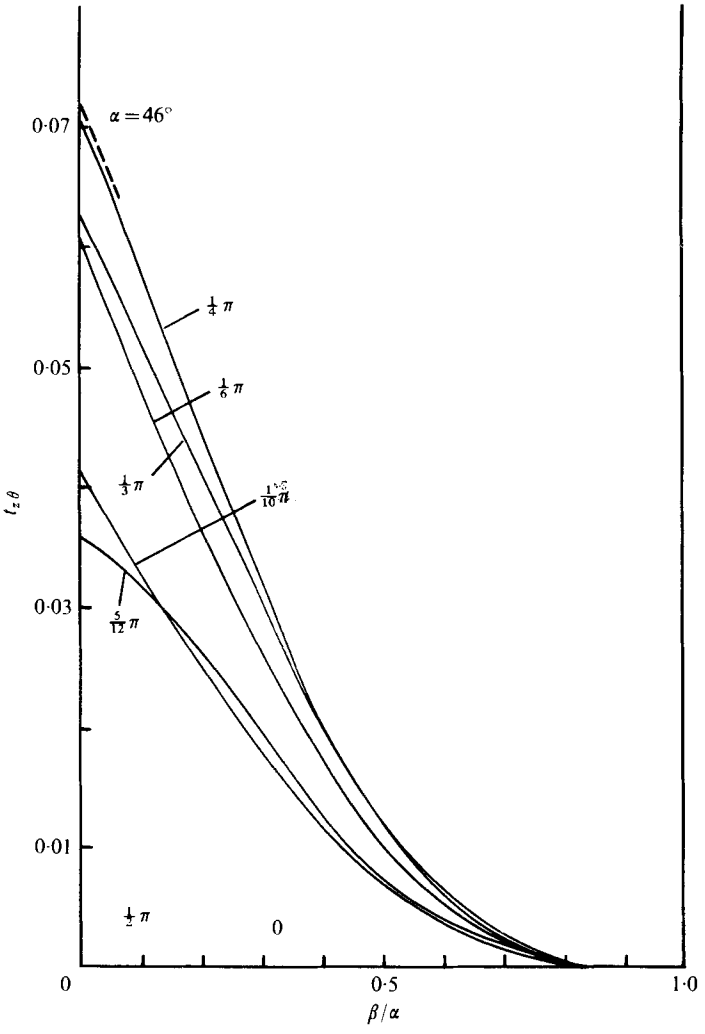

FIGURE 11. Graph of $t_{z\theta}$ given by (4.13) for various α. Maximum value is attained at $\alpha = 46°$ on the bisector.

respect to the translational motion of a sphere, and so it becomes zero in the following cases: (i) when a sphere lies on the bisector and moves either perpendicular to the bisector or perpendicular to the intersection of the wedge, (ii) when the wedge angle reduces to zero (i.e. two parallel plane walls) and a sphere moves parallel to or perpendicular to the walls at an arbitrary position, and (iii) when a sphere lies very close to one of the walls and moves parallel to or perpendicular to it. These are special cases of more general ones; other possibilities of vanishing side force are considered in the next section. The torque on the sphere is directed only in the z direction, and its magnitude becomes zero as the sphere approaches one of the walls.

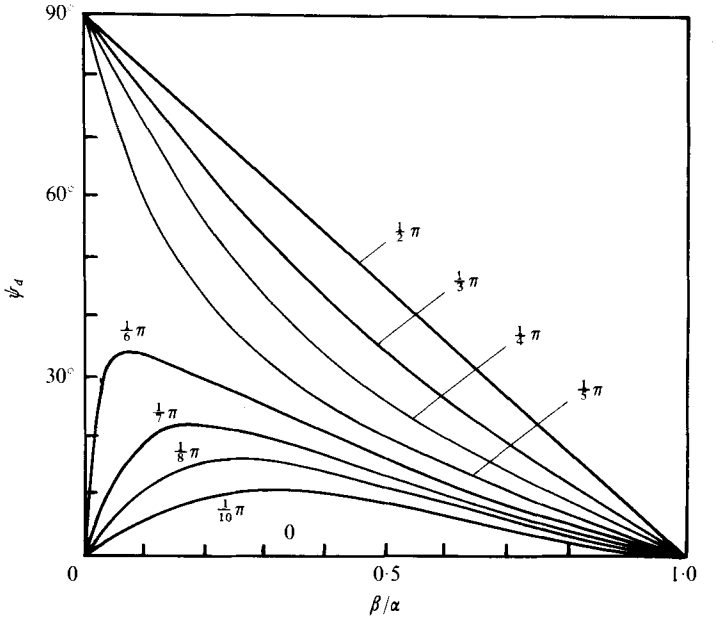

FIGURE 12. One of the principal axes of translation $\gamma = \psi_d$ for various α. The other one is in the direction $\gamma = \psi_d + \frac{1}{2}\pi$, and the third one is perpendicular to both of them.

5. Principal axes and a torque-free direction

In the foregoing sections, we have obtained the force and torque acting on the sphere in the form

$$\mathbf{F} = -6\pi\mu a[\mathbf{I} + \epsilon\mathbf{K} + O(\epsilon^2)] \cdot \mathbf{V}, \tag{5.1}$$

$$\mathbf{T} = -8\pi\mu a^2[\epsilon^2\mathbf{C} + O(\epsilon^4)] \cdot \mathbf{V}, \tag{5.2}$$

where

$$\mathbf{K} = \begin{pmatrix} f_{rr} & f_{r\theta} & 0 \\ f_{\theta r} & f_{\theta\theta} & 0 \\ 0 & 0 & f_{zz} \end{pmatrix}, \quad \mathbf{C} = \begin{pmatrix} 0 & 0 & t_{rz} \\ 0 & 0 & t_{\theta z} \\ t_{zr} & t_{z\theta} & 0 \end{pmatrix} \tag{5.3}$$

are termed the wall-effect tensors. Note that in general the tensor $\mathbf{K}$ is symmetric, i.e. $f_{r\theta} = f_{\theta r}$, but that the tensor $\mathbf{C}$ is not necessarily symmetric, which is the case in our results.

5.1. *Principal axes of translation*

As an immediate consequence of the properties of symmetric tensors, there exist three mutually perpendicular axes along which the particle translates without undergoing a side force (principal axes of translation). We shall now seek these principal axes and principal drags (i.e. the forces exerted on the sphere when it moves in these directions), which correspond to the eigenvectors and eigenvalues of the tensor $\mathbf{K}$, respectively. The principal drags are

$$6\pi\mu a[1 + \epsilon\lambda_n + O(\epsilon^2)]\,|\mathbf{V}| \quad (n = 1, 2, 3), \tag{5.4}$$

where

$$\lambda_1 = \tfrac{1}{2}(f_{rr} + f_{\theta\theta}) + [\tfrac{1}{4}(f_{rr} - f_{\theta\theta})^2 + f_{r\theta}^2]^{\frac{1}{2}},$$
$$\lambda_2 = f_{rr} + f_{\theta\theta} - \lambda_1,$$

and

$$\lambda_3 = f_{zz}. \tag{5.5}$$

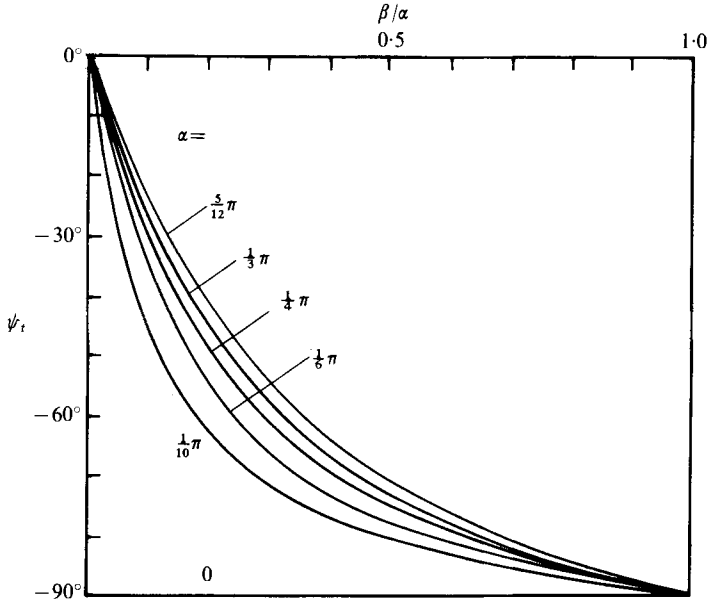

FIGURE 13. Torque-free direction ψ_t defined by (5.7).

The last is a translation parallel to the z axis, and the first two are motions in the directions

$$\gamma = \psi_d + \tfrac{1}{2}n\pi \quad (n = 0, 1), \tag{5.6}$$

where

$$\psi_d = \tfrac{1}{2}\tan^{-1}[2f_{r\theta}/(f_{rr} - f_{\theta\theta})].$$

Numerical values of ψ_d as a function of α and β are shown in figure 12. It is to be noted that there exists a critical angle between $\frac{1}{6}\pi$ and $\frac{1}{5}\pi$, where the principal axes change their directional tendencies.

5.2. *Torque-free direction*

There exists only one direction of motion along which the sphere does not experience a torque up to the present order of approximation. This line is in the direction $\gamma = \psi_t$ on the $z = 0$ plane, where

$$\psi_t = -\tan^{-1}(t_{zr}/t_{z\theta}). \tag{5.7}$$

Numerical values of ψ_t as a function of α and β are shown in figure 13. This direction does not in general coincide with any of the principal axes of translation.

6. Another expression for the wall effect

So far we have been discussing the wall effect on the force and torque experienced by a sphere, the values of which are of the form ϵf and $\epsilon^2 t$, respectively. In these expressions, we take the minimum distance d between the sphere and the walls as a characteristic length. Since the parameter ϵ itself is a function of the particle position, it is not convenient to see how the total wall corrections depend on the location of the sphere, when its angular position varies from one wall to the other, keeping the

α	$\frac{1}{2}\pi$	$\frac{1}{3}\pi$	$\frac{1}{4}\pi$	$\frac{1}{6}\pi$
C_{rr}	0	1·4179	4·5769	16·358
$C_{r\theta}$	0	0·67020	2·4986	11·067
C_{zz}	0	0·32641	1·3085	6·4487

TABLE 1. Values of C_{rr}, $C_{r\theta}$ and C_{zz}.

α	$\frac{1}{3}\pi$	$\frac{1}{4}\pi$	$\frac{1}{6}\pi$	$\frac{1}{10}\pi$
C_{zr}	0·70895	2·2885	8·1792	33·363
$C_{z\theta}$	0·33511	1·2493	5·5340	29·084
$-C_{rz}$	0·16321	0·65427	3·2243	18·715
$-C_{\theta z}$	0·23414	1·0273	5·3661	32·130

TABLE 2. Values of C_{zr}, $C_{z\theta}$, C_{rz} and $C_{\theta z}$.

distance from the intersection constant. Therefore we introduce another expression for the force and torque, $\epsilon^* f^*$ and $\epsilon^{*2} t^*$, respectively, where f^* and t^* are given by†

$$f^* = f/\sin|\alpha-\beta|, \quad t^* = t/\sin^2(\alpha-\beta), \tag{6.1}$$

so that $\epsilon^* = a/\rho$ remains constant, where ρ is the distance between the sphere and the intersection of the walls. Careful calculation (Sano 1977) shows that f^*_{rr} generally takes a minimum value on the bisector, however it takes a minimum value at a certain point between the wall and the bisector when the semi-vertex angle α lies in the range $\frac{1}{5}\pi < \alpha < \frac{1}{2}\pi$. Also one of the principal drags λ^*_2 has a minimum value at an intermediate position for $\frac{1}{9}\pi \lesssim \alpha \lesssim \frac{1}{5}\pi$. The function $f^*_{r\theta}$ takes the value 0 on the bisector, decreases like $-\beta/\alpha$ and asymptotes to $-\frac{9}{16}$ as one of the walls is approached. Other functions f^* and λ^* take minimum values on the bisector, and increase monotonically in proportion to $(1-\beta/\alpha)^{-1}$ as β/α tends to unity.

The asymptotic behaviours of the f^* as the sphere approaches one of the walls are

$$\left.\begin{aligned} f^*_{rr} &= \kappa^{-1}[\tfrac{9}{16}+\tfrac{21}{32}\kappa^2+C_{rr}(\alpha)\,\kappa^3+O(\kappa^4)], \quad f^*_{r\theta} = -\tfrac{9}{16}+\tfrac{9}{32}\kappa^2+C_{r\theta}(\alpha)\,\kappa^3+O(\kappa^4), \\ f^*_{\theta\theta} &= \kappa^{-1}[\tfrac{9}{8}-\tfrac{3}{8}\kappa^2+O(\kappa^4)], \quad f^*_{zz} = \kappa^{-1}[\tfrac{9}{16}+\tfrac{3}{32}\kappa^2+C_{zz}(\alpha)\,\kappa^3+O(\kappa^4)], \end{aligned}\right\} \tag{6.2}$$

where $\kappa = \alpha-\beta$, and the coefficients C are tabulated in table 1. The values of f^* and λ^* calculated by the use of these formulae are accurate to 2% even for $\beta/\alpha = 0{\cdot}7$. The functions $|t^*_{\theta z}|$ and $t^*_{z\theta}$ become maximum on the bisector, gradually decreasing to zero like $(1-\beta/\alpha)^2$ as one of the walls is approached; on the other hand $|t^*_{rz}|$ and t^*_{zr} take the value 0 on the bisector, increase like β/α, become maximum at a certain intermediate position and finally decrease like $(1-\beta/\alpha)$ in the vicinity of the wall. The asymptotic forms of the t^* near the wall are

$$\left.\begin{aligned} t^*_{zr} &= C_{zr}(\alpha)\,\kappa+O(\kappa^2), \quad t^*_{z\theta} = C_{z\theta}(\alpha)\,\kappa^2+O(\kappa^3), \\ t^*_{rz} &= C_{rz}(\alpha)\,\kappa+O(\kappa^2), \quad t^*_{\theta z} = C_{\theta z}(\alpha)\,\kappa^2+O(\kappa^3), \end{aligned}\right\} \tag{6.3}$$

where the values of C's are given in table 2.

† Copies of the tables of f^* and t^* are available to interested readers on request to the authors.

The apparent loss of symmetry in the functions f, λ and t with respect to the argument β, which leads to the presence of the cusps at $\beta = 0$ except for the case $\alpha = \frac{1}{2}\pi$, arises from our definition of ϵ, so that the symmetries (or antisymmetries) reappear in our new expressions for f^*, λ^* and t^* given in this section.

7. Discussion

We have been confining our attention to the first-order effect of the boundary wall. As far as the approximation to this order is concerned, the present analysis could be applied to more general situations. According to Brenner (1962, 1964), the hydrodynamic force **F** experienced by any non-spherical particle can be evaluated by combining the present results for **K** and the knowledge of the Stokes force $\mathbf{F}_0$ on the same particle moving at the velocity **V** in an *unbounded* domain:

$$\mathbf{F} = [\mathbf{I} - \mathbf{S}_0 . \mathbf{K} c/d + o(c/d)]^{-1} . \mathbf{F}_0, \tag{7.1}$$
$$\mathbf{F}_0 = -6\pi\mu c \mathbf{S}_0 . \mathbf{V},$$

where c is a characteristic dimension of the particle and $\mathbf{S}_0$ is the so-called Stokes translation tensor for the corresponding particle. Furthermore if the fluid itself is not at rest at infinity, the modification required is solely to replace the particle velocity **V** by the velocity difference $\mathbf{V} - \mathbf{V}_P^b$, where $\mathbf{V}_P^b$ is the background velocity at P in the absence of that particle. However, no such direct extensions could be made for the torque exerted on a non-spherical particle in the presence of boundary walls, because they depend on the shape as well as the orientation of that body at the same order ϵ^2 as is treated in this paper.

When the sphere is allowed to rotate, one of the boundary conditions (2.3c) should be replaced by

$$\mathbf{v} = \mathbf{V} + \boldsymbol{\omega} \times \mathbf{R} \quad \text{on the surface of the sphere,} \tag{7.2}$$

where **R** is the position vector with its origin at P, and the angular velocity $\boldsymbol{\omega}$ is determined through the condition of zero torque. The equations of motion as well as the boundary conditions are linear, so we can deal separately with translation and rotation of the sphere. The direction of the force induced by a rotation which itself is a result of translation is either parallel to the z axis for the case considered in § 3 or confined in the $z = 0$ plane for the case considered in § 4. In addition the contribution of the rotation to the induced velocity is at most of order $\epsilon^2 |\boldsymbol{\omega}| a$.† If the sphere translates at a given velocity **V**, it will undergo a torque of order $\epsilon^2 |\mathbf{V}|$ which will make the sphere rotate with angular velocity $\boldsymbol{\omega}$ of order $\epsilon^2 |\mathbf{V}|/a$, which in turn gives the correction of order $\epsilon^4 |\mathbf{V}|$ to the translational velocity. Thus our analysis, although developed for the induced force without rotation, remains unchanged even if the sphere is allowed to rotate freely. Moreover it also predicts the angular velocity of the sphere $\boldsymbol{\omega}$ by the relation

$$\boldsymbol{\omega} = -\epsilon^2 \mathbf{C} . \mathbf{V}/a, \tag{7.3}$$

as far as the lowest-order approximation is concerned.

† As a matter of fact the force $\mathbf{F}_{\text{rot}}$ induced by the rotation of a sphere with angular velocity $\boldsymbol{\omega}$ is (Happel & Brenner 1973, p. 171)

$$\mathbf{F}_{\text{rot}} = -8\pi\mu a^2 \epsilon^2 \mathbf{D} . \boldsymbol{\omega},$$

where **D** is the transpose of **C** given by (5.3).

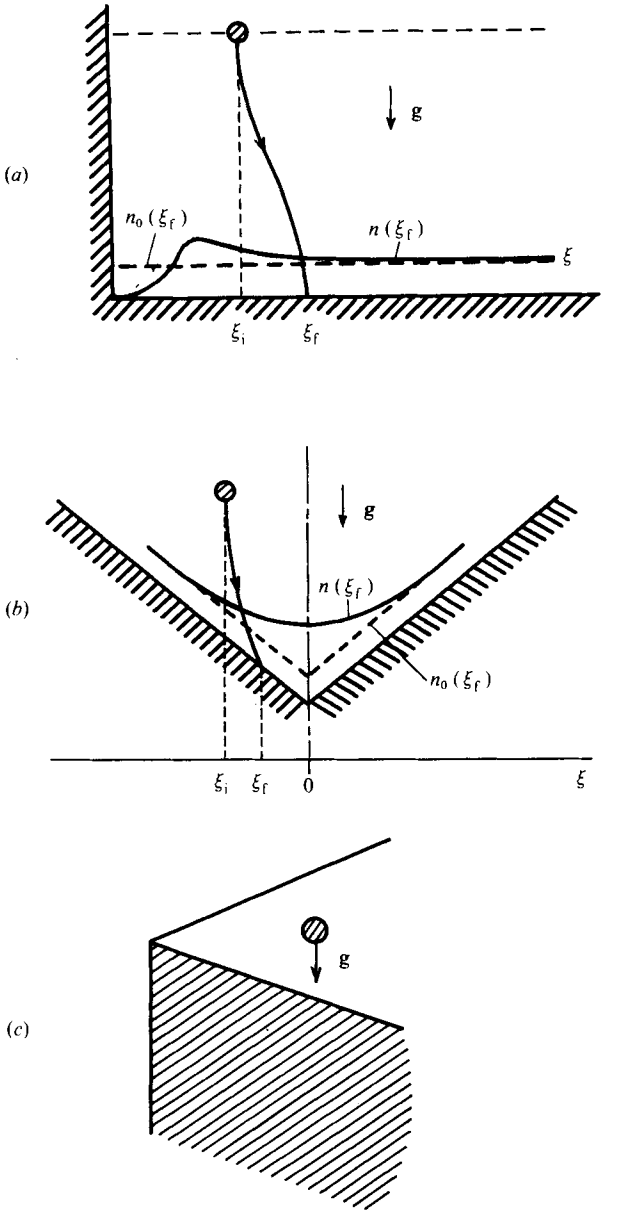

FIGURE 14. Sedimentation of a sphere, where ξ_i and ξ_f represents the initial and final horizontal positions of the sphere, respectively.

The present analysis thus extended may be used as a basis for some predictions. First let us consider the sedimentation of a particle in the cases illustrated in figure 14. In figures 14 (*a*) and (*b*), we denote the initial and final position of the sphere by ξ_i and ξ_f, respectively. (Gravity acts in the direction shown by the arrow labelled $\mathbf{g}$.) Then owing to the side-force found in our calculation, we find

$$\xi_i \leqslant \xi_f \qquad \text{for case } (a),$$

and

$$\xi_i \leqslant \xi_f \leqslant 0 \text{ or } 0 \leqslant \xi_f \leqslant \xi_i \qquad \text{for case } (b).$$

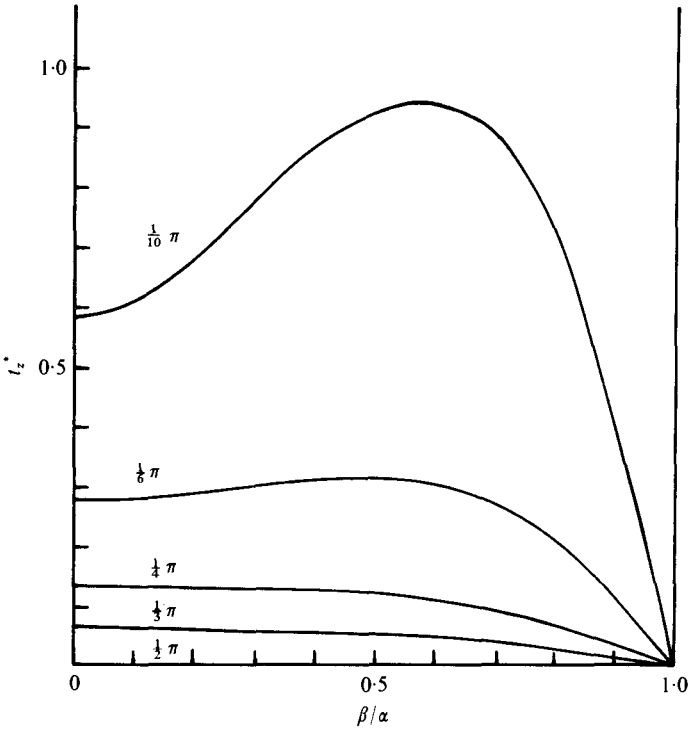

FIGURE 15. Graph of $t_z^* = (t_{rz}^{*2} + t_{\theta z}^{*2})^{\frac{1}{2}}$, for various α, where $\epsilon^{*2} t_z^*$ is the torque acting on the sphere translating parallel to both walls without rotation.

Using these findings, we now examine the statistical distribution of sedimenting particles on the bottom wall. When the interaction among particles is neglected as in a dilute suspension, we can replace the sedimentation of many particles by the ensemble of the sedimentation of one particle, in which the particle is released randomly at a certain distance from the bottom. Then we shall have a statistical distribution for the number of spheres $n(\xi_f)$ starting from the same horizontal plane and reaching the bottom wall at $\xi = \xi_f$ similar to the one shown by the solid line, where we also show by the dashed line the distribution $n_0(\xi_f)$ which would come out in the absence of the wall effect. The third example is the motion of the sphere falling under gravity in the presence of two vertical intersecting walls (figure 14(*c*)). As has been shown in § 3, the sphere will translate with slightly reduced velocity the amount of which is evaluated in terms of f_{zz}. It will also undergo rotation in the direction illustrated in figure 6 with the angular velocity shown in figure 15, except for a constant numerical factor.

This work was partially supported by the Grant-in-Aid for Scientific Research from the Ministry of Education.

REFERENCES

BRENNER, H. 1962 *J. Fluid Mech.* **12**, 35.

BRENNER, H. 1964 *J. Fluid Mech.* **18**, 144.

BRENNER, H. & HAPPEL, J. 1958 *J. Fluid Mech.* **4**, 195.

ERDÉLYI, A., MAGNUS, W., OBERHETTINGER, F. & TRICOMI, F. G. 1954 *Tables of Integral Transforms*, vol. 2. McGraw-Hill.

FAXÉN, H. 1921 Dissertation, Uppsala University (see Happel & Brenner 1973).

FAXÉN, H. 1922 *Ann. Phys.* **68**, 89.

HAPPEL, J. & BRENNER, H. 1973 *Low Reynolds Number Hydrodynamics*. Noordhoff.

HASIMOTO, H. 1976 *J. Phys. Soc. Japan* **41**, 2143; **42**, 1047.

HO, B. P. & LEAL, L. G. 1974 *J. Fluid Mech.* **65**, 365.

IMAI, I. 1973 *Ryutai Rikigaku* (*Fluid Dynamics*). Syokabo.

KIM, M. U. 1976 Ph.D. thesis, University of Tokyo.

LADENBURG, R. 1907 *Ann. Phys.* **23**, 447.

LORENTZ, H. A. 1907 *Abh. Theor. Phys., Leipzig* **1**, 23.

SANO, O. 1977 Ph.D. thesis, University of Tokyo.

SANO, O. & HASIMOTO, H. 1976 *J. Phys. Soc. Japan* **40**, 884.

SANO, O. & HASIMOTO, H. 1977 *J. Phys. Soc. Japan* **42**, 306.

WAKIYA, S. 1956 *Res. Rep. Fac. Engng, Niigata Univ.* (*Japan*) **5**, 1.